ASAP1 promotes tumor progression and angiogenesis and independently predicts poor prognosis and lymph node metastasis of gastric cancer

Hongyu Gao
Tumor Hospital of Harbin Medical University
Ling Qin
Tumor Hospital of Harbin Medical University
Huawen Shi
Tumor Hospital of Harbin Medical University
Hongfeng Zhang
Tumor Hospital of Harbin Medical University
Chunfeng Li
Tumor Hospital of Harbin Medical University
Yan Ma
Tumor Hospital of Harbin Medical University
Haibin Song
Tumor Hospital of Harbin Medical University
Zhiguo Li
Tumor Hospital of Harbin Medical University
Yingwei Xue (xyw_801@163.com)
Tumor Hospital of Harbin Medical University https://orcid.org/0000-0001-6006-0898
Tianbo Liu
Tumor Hospital of Harbin Medical University

Research

Keywords: Gastric cancer, ASAP1, prognosis, metastasis, angiogenesis, epithelial-mesenchymal transition

Posted Date: December 3rd, 2019

DOI: https://doi.org/10.21203/rs.2.17932/v1

Abstract

Background: Although ArfGAP with SH3 Domain, Ankyrin Repeat and PH Domain 1(ASAP1) is involved in the development of various malignancies, its clinical significance and mechanism in gastric cancer (GC) remains unclear.

Methods: The effects of ASAP1 on tumor progression, angiogenesis, and epithelial-mesenchymal transition were evaluated in vitro. The effects of ASAP1 on tumor growth and angiogenesis were also explored in vivo. The Cancer Genome Atlas (TCGA) and Gene Expression Omnibus (GEO) databases were used to gather ASAP1 expression data.

Results: It showed that ASAP1 expression strongly correlated with the TNM stage ($P < 0.0001$) and lymph node metastasis ($P < 0.0001$). Multivariate analyses indicated that ASAP1 overexpression ($P < 0.0001$) was an independent predictor for overall survival in patients with GC. Moreover, the results revealed that ASAP1 overexpression was independently related to lymph node metastasis ($P = 0.0001$). ASAP1 knockdown inhibited tumor cell motility, migration, invasion, and angiogenesis, which was accompanied with the downregulation of metastatic and angiogenic biomarkers. Furthermore, ASAP1 inhibition resulted in the simultaneous downregulation of mesenchymal markers and upregulation of epithelial markers. In addition, ASAP1 promoted tumor growth and angiogenesis in the xenograft mice model. The combined datasets (TCGA and GEO) suggested that ASAP1 was associated with malignant behavior of tumor and tumor invasion, metastasis, and angiogenesis.

Conclusion: To our knowledge, our study is the first to reveal that ASAP1 promotes tumor progression and angiogenesis, and indicates a prognostic potential in GCs.

Background

Gastric cancer (GC), which ranks fifth in terms of morbidity, accounts for approximately 8% of newly diagnosed cancers [1]and is still the third most common reason for cancer-related deaths worldwide [2]. GC frequently occurs in Eastern Europe, Asia, and the Middle and South America [3]. GC is the third most common malignancy in China, and approximately 380,000 newly diagnosed cases are reported every year [4].Conventional therapeutic options for GC include surgery, radiotherapy, and chemotherapy. However, approximately 40–60% of GC cases will develop tumor metastasis or recurrence following radical surgery [5,6], with a consequently poor prognosis [7]. The diagnostic and treatment methods for GC have been improved recently, but the 5-year survival of patients with GC remains <30% [8] and is even particularly worse for more advanced stages [9,10]. Therefore, reliable prognosis markers are urgently needed for the diagnosis, prediction of poor prognostic outcome, and enhancement of relapse and metastasis prediction for patients with GC.

ArfGAP with SH3 Domain, Ankyrin Repeat and PH Domain 1 (ASAP1), also referred to as AMAP1 or DDEF1, is positioned on 8Q24.21-Q24.22, and it is constituted by 37 exons, which is 125 kDa in terms of molecular mass. It affects cell spreading and cell migration by remodeling actin cytoskeleton [11–14]

and regulating the membrane traffic in cells [14]. ASAP1 can also regulate cell adhesion by binding with Src and CrkL via a domain rich in proline, together with the focal adhesion kinase (FAK) via the SH3 domain [11,15,16]. Furthermore, ASAP1 plays a vital role in the regulation of tumor cell invasion, motility, and metastasis [17,18]. Correspondingly, ASAP1 overexpression has frequently occurred as a factor predicting the malignancy of various caners, such as colorectal cancer (CRC), breast cancer (BC), prostate cancer (PCa), uveal melanomas, ovarian cancer, and neck and head cancer [13,19–23]. However, the clinically predictive significance of ASAP1 and its underlying mechanism in GC have not been explored.

ASAP1 may potentially participate in tumor genesis and progression. Therefore, this study aimed to explore the effect of ASAP1 on GC cells as well as tissues and to define its clinical significance and function of promoting angiogenesis as well as the epithelial-mesenchymal transition (EMT) apart from migration and invasion.

Methods

Cases and samples

Clinical specimens had been collected based on 625 consecutive GC cases confirmed histologically and 30 normal tissue samples who were surgically treated at Harbin Medical University Cancer Hospital between January 2007 and December 2011. The primary lesions, metastatic lymph nodes together with peritoneum were matched in 30 primary GC patients. Additionally, fresh tissue specimens were collected from 40 cases, which had included the metastatic tissue specimens (n = 10), primary tumor tissue specimens without metastasis (n = 10), primary tumor tissue specimens with metastasis (n = 10), and paired adjacent normal tissue specimens (n = 10), which were preserved at −80 ℃ immediately following resection for protein as well as RNA extraction. No case had received radiotherapy or chemotherapy before surgical treatment. Tumor stage would be determined in accordance with the American Joint Committee on Cancer criteria [24].

Table 1 displays the clinicopathological features for 625 GC cases. As could be seen, the median age of these patients was 58 years (range, 27–82 years). The length of follow-up would be determined to be the duration from the diagnosis date to the date of death or the final follow-up. The current study had gained approval from the Medical Ethics Committee of Harbin Medical University Cancer Hospital. Each patient had submitted the informed consent for participation.

Tissue microarrays

GC tissue microarray (TMAs) was described as following. In short, the tissue array device would be utilized to generate the holes in one receptive paraffin mass and to obtained the tissue core based on the donor tissue mass through the thin-walled needle (2 mm in inner diameter) supported under the X-Y precision guidance. Moreover, core samples would be recovered from selective donor region for direct extrusion to receptive mass at the defined microarray coordinates. Additionally, a solid steel wire tightly fit

within the tube would be utilized for tissue core transfer to the receptive mass. Following constructing the array mass, each tissue mass would be sliced using the microtome into sections 4 μm in thickness, followed by fixation onto the slide. Masses collected based on 625 pairs of surgically resected GCs as well as corresponding normal gastric samples of patients would be arrayed to be the triplicate spots on slides, with the diameter of 2 mm.

Immunohistochemical staining and evaluation

ASAP1 immunohistochemistry (IHC) had been carried out by the Two-Step IHC Detection Reagent (PV–6001) kit (Zhong Shan Golden Bridge Biological Technology Inc., Beijing, China) in strict accordance with manufacturer protocol. Afterwards, the paraffin-embedded slides comprising of the gastric samples would be sliced using the microtome (4 μm in thickness) for IHC. Briefly, each tissue section would be subjected to deparaffinage with xylene and rehydration using gradient alcohol solutions following the normalized procedure. Later, sections would be subjected to 10 min of immersion within 3% hydrogen peroxide, so as to get rid of tje endogenous peroxidase. Then, 2 min of antigen retrieval would be carried out within the pressure cooker supplemented with citrate buffer (10 mmol/L, pH 6.0) for enhancing the immune reactivity. Sections would then be subjected to incubation with a polyclonal rabbit antibody against ASAP1 (1:150 dilution; Abcam) at 4 °C overnight. Then, sections were washed with PBS (3×5 min), followed by 20 min of incubation with secondary antibody (300–500 ml) under ambient temperature. Then, the sections were washed with PBS (3×5 min), colour would be developed using 3,3’-diaminobenzidine tetrahydrochloride (Dako, Hamburg, Germany), and then all slides would be subjected to mild counterstaining using hematoxylin, followed by examination under the light microscope.

ASAP1 level was determined through combining the proportion as well as intensity of tumor cells under positive staining. The proportion would be divided into several grades: 0 (0%), 1 (0–10%), 2 (11–50%), 3 (51–70%), and 4 (>71%). The intensity was also scored as follows: 0 (negatively stained), 1 (weakly stained), 2 (moderately stained), and 3 (intensely stained). The eventual ASAP1 expression score would be the sum of the two scores, which was within the range of 0–7. To carry out statistical analysis, patients with the eventual score of < 4 were classified into low expression group; otherwise, they were classified into high expression group.

Two pathologists blinded with the clinical and pathological data would independently rate the staining intensity of all samples. At last, results of staining assessed and tumors allocated by these two pathologists were identical. Any discrepant case would be reviewed by these two pathologists again and a senior pathologist at the same time to reach a consensus.

Cell lines as well as culture

Human GC cell lines, including BGC–823, MGC–803 and SGC–7901, together with human gastric epithelial cell line GES–1, had been provided by American Type Culture Collection (ATCC, Manassas, VA),

and the short tandem repeat profiling was employed 3 months prior to the beginning of the current study, so as to guarantee the authenticity of the cell lines. No additional authentication was carried out by the authors in the study period. We selected MGC–803 and SGC–7901 cell lines that had high ASAP1 expression to carry out the siRNA knockdown tests for the following analyses. In addition, MGC–803 as well as SGC–7901 cell line would be maintained within RPMI–1640 medium (Gibco BRL, Carlsbad, CA, USA) containing 10% fetal bovine serum (FBS; Gibco BRL), penicillin (100 units/mL) and streptomycin (100 μg/mL) under humid 5% CO_2 atmosphere at 37 °C.

Western blotting

Total protein had been separated using the RIPA buffer supplemented with 1% mixture of protease inhibitor. Later, the mixture would be subjected to 15 min of centrifugation at 12 000 g and 4 °C, and supernatants were collected. Thirty micrograms of the protein extract would then be separated through 10% SDS polyacrylamide gel electrophoresis (PAGE), followed by transfer onto the PVDF membrane (Millipore Company, USA). Later, the membrane had been subjected to blocking and incubation with antibodies against target proteins. Primary antibodies, anti-ASAP1, anti-MMP2, anti-MMP–9, VEGF, HIF–1□, Vimentin, N-cadherin, E-cadherin, Fibronectin, Snail, as well as Twist had been diluted with buffer and adopted to incubate overnight at 4 °C, followed by incubation using secondary antibody. β-actin served as the gel loading control, and the experiment had been repeated for three times.

Real-time RT-PCR

Total RNA had been extracted based on cells as well as tissues by the TRIzol reagent (Invitrogen Life Technologies, Carlsbad, CA, USA). 500 ng RNA would then be reversely transcribed into cDNA by the iScript reverse transcription kit (BioRad, Hercules, CA, USA). ASAP1 primers had been designed, including 5’-AGGCAGACAACGATGACGAG–3’ (forward), and 5’-AAAGGACACTGGAAAGACCC–3’ (reverse). Notably, β-actin served as an internal reference, with the primers shown below: 5’-CTTAGTTGCGTTACACCCTTTCTTG–3’ (forward), and 5’- CTGTCACCTTCACCGTTCCAGTTT–3’ (reverse). The amplification conditions were as follows: at 95 °C for 10 min; at 95 °C for 10 s, at 60 °C for 20 s as well as at 72 °C for 30 s for 40 cycles. All experiments had been carried out for three times under identical reaction conditions.

Cell motility and migration assay

The migration of cells had been evaluated through detecting cell movement in one scraped cell area made by the 200 μL pipette. Cells were seeded in the six-well plates, followed by starvation within the serum-free medium containing mitomycin C (1 μg/ml) overnight. Then, the rest cells would be rinsed by PBS for removing the cell debris, followed by incubation at 37 °C under humid 5% CO_2 atmosphere using the serum-free medium. In addition, the closure of wound would be monitored at 0 as well as 24 h,

respectively. Images of cells migrating to cell-free scratch area had been obtained, meanwhile, cell migration distance would be determined using the inverted microscope. The width of scratch was measured through the percentage relative to the untreated control cells. All experiments were performed for three times independently.

Cell invasion trial

The upper polycarbonate membrane surface (with the pore size of 8 μm) within the Transwell filter insert (Costar, Pleasanton, CA, USA) had been covered by 60–80 μL Matrigel (3.9 μg/μL). Then the membrane was incubated at 37 °C for 30 min, and the Matrigel was solidified, which was subsequently used as the extracellular matrix (ECM) to analyze the invasion of tumor cells. Cells would be collected into the serum-free growth medium (100 μL) before they were inoculated to the upper chamber compartment. Cells migrating to the pores within the inserted filter from the Matrigel would be subjected to 30 min of fixation by 100% methanol. Afterwards, cells on lower membrane surface would be subjected to 20 min of crystal violet staining. Eventually, the invaded cell numbers would be calculated within five randomly chosen fields of view (FOV) using a microscope. All experiments had been carried out independently three times.

Tube formation experiment in vitro

The angiogenesis assay in vitro assay had been performed within the 96-well plates covered by ECMatrix^{TM} (50 μl, BD Biosciences) in accordance with manufacturer protocol. Typically, the tube formation experiment was carried out on the basis of the 3D capillary-like tubular structure formation capacity of endothelial cells cultivated onto the basement membrane extract gel. Prior to the experiment, Matrigel Basement Membrane Matrix (100 μl, BD Biosciences) would be added into the 24-well plate, followed by 30 min of incubation at 37 ℃. Then, human umbilical vein endothelial cells (HUVECs) would be resuspended into the harvested supernatants of ASAP1-siRNA, control, as well as negative control groups, separately. Afterwards, 2×10^4 HUVECs would be inoculated onto the polymerized Matrigel layer, followed by 24 h of incubation at 37℃. Then, the connecting branch number between cells was counted to analyze the formation of lumens in the above HUVECs. All experiments were carried out for at least three times.

Xenograft models

SGC–7901 cells (5×10^6cells/ml) stably transfected with siRNA (ASAP1) or control vector were subcutaneously injected into 4-week-old BALB/C nude mice. Then, the growth of tumor would be observed every week through detecting tumor diameter at perpendicular direction (length (L) as well as width (W)) using the Vernier caliper. The tumor volume (V) would be determined according to the formula: $V = LW^2/2$.

Database analysis

The data of ASAP1 expression were downloaded from The Cancer Genome Atlas (TCGA; https://cancergenome.nih.gov/) database, which contained 384 tumor samples and 37 normal samples. In addition, ASAP1 expression data (GSE55696) for gastric tissues were downloaded from the public Gene Expression Omnibus (GEO; https://www.ncbi. nlm.nih.gov/geo/) database, which contained 19 chronic gastritis, 19 low-grade intraepithelial neoplasia of stomach, 20 high-grade intraepithelial neoplasia stomach, and 19 early gastric cancer samples. The relationships of ASAP1 with cancer hallmark genes [25] on behalf of tumor invasion, metastasis and angiogenesis were analyzed.

Statistical methods

The SPSS (SPSS 13.0, Chicago, IL, USA) was adopted for all statistical analyses. The relationship of ASAP1 level with the clinicopathological characteristics would be assessed by Chi-square or Fisher's test. Survival curves were plotted by The Kaplan–Meier method was employed to plot the survival curves, which were then compared using log-rank test. Each variable with significance upon univariate analysis was performed multivariate survival analysis by Cox regression model. The association of ASAP1 protein expression with lymph node metastasis (LNM) would be evaluated through univariate as well as multivariate logistic regression analysis. Continuous data were displayed in the form of mean ± standard deviation (SD). Moreover, differences between two groups would be examined through the student's test, while those in multiple groups would be assessed using the one-way ANOVA. A two-sided difference of $P < 0.05$ would be deemed with statistical significance.

Results

ASAP1 expression in GC tissues and cell lines

Western blot analysis was applied to examine the expression of ASAP1 protein in fresh frozen tumor and normal tissues. ASAP1 was detected as a band of 120~130 kDa. It revealed that ASAP1 protein expression gradually increased from normal tissue to primary tumor tissues without metastasis, and to those with metastasis. The statistical differences between each group were observed in *Supplementary Figure 1A.* However, its expression in metastastic lesion inversely declined compared that in primary lesion which came from the same tissue. Expression of ASAP1 mRNA was also examined using real-time RT-PCR. And these results are similar to the western blot's displayed in *Supplementary Figure 1B.* IHC method demonstrated that ASAP1 was obviously localized to the cytoplasmic compartment of tumor cells (*Supplementary Figure 1C).*. ASAP1 was highly expressed in 36.3% of GC cases (227/625). Geographic differences were also observed in ASAP1 cytoplasmic staining (*Supplementary Figure 1C),*, which was more intense in the primary foci than that in the invasive foci among the same patients.

ASAP1 expression levels in human gastric epithelial cell line GES–1 and three different GC cell lines: MGC–803, BGC–823, and SGC–7901 were evluated using western blot and real-time RT-PCR analyses. MGC–803 cell line presents the highest ASAP1 expression level compared with normal GES–1 cell line and other two GC cell lines (*Supplementary Figure 2A,B).*. It indicated the highest ASAP1 knock-down efficiency among the transfection groups in both MGC–803 and SGC–7901 cells (*Supplementary Figure 2C,D),*, thus applying for the following experiments.

Relationships of ASAP1 protein expression with clinicopathologic characteristics in GCs

In *Table 1,* elevated ASAP1 expression positively correlated with TNM stage ($P < 0.0001$) and lymph node metastasis ($P < 0.0001$). But, there was no significant association between ASAP1 and age, gender, main location, tumor size, depth of invasion, Borrmann grouping, lauren classification, and resectability.

Effect of ASAP1 protein expression level on metastasis of lymph node

Univariate analysis showed that the metastasis of lymph node was strongly related with tumor size ($P = 0.001$), TNM stage ($P < 0.0001$), depth of invasion ($P < 0.0001$), Borrmann grouping ($P = 0.018$), lauren classification ($P = 0.001$), and resectability ($P < 0.0001$) in *Supplementary Table 1.* To assess the independent predictive value of ASAP1 expression for lymph node metastasis (*Figure 1A),*, multivariate logistic regression analysis (*Table 2)* demonstrated that ASAP1 increased expression was an independent predictor for lymph node metastasis in GC ($P = 0.0001$; odds ratio [OR], 3.005; 95% confidence interval [CI], 1.734–5.383).

ASAP1 protein expression predicts survival in GC patients

The Kaplan-Meier survival curves of ASAP1 for overall survival (OS) are shown in *Figure 1C.* The 5-year OS rates of 625 GC patients and 490 GC patients with R0 resection were 55.2% and 66.1%, respectively. Univariate analysis revealed that age, main location, tumor size, TNM stage, Borrmann grouping, lauren classification, resectability, depth of invasion, lymph node metastasis, and ASAP1 expression were correlated with survival outcomes. However, gender had no affect on OS. The multivariate analysis demonstrated that age, TNM stage, main location, Borrmann grouping, resectability, depth of invasion, lymph node metastasis, and ASAP1 overexpression were also independent predictors for OS in 625 GC patients (data not shown in Tables).

To exclude the effect of resectability on prognosis, we further analyzed the survival of 490 GC patients after R0 resection. The multivariate analysis showed in *Supplementary Table 2* indicated that ASAP1 increased expression was an independently predictor for OS in GCs with R0 resection ($P < 0.0001$). Other

parameters such as TNM stage, depth of invasion, lymph node metastasis, and Borrmann grouping were also independently associated with OS (P = 0.019, P = 0.001, P = 0.030, and P = 0.002).

ASAP1 knockdown inhibits cell motility, migration, and invasion

For cancer metastasis, cell motility, migration, and invasion are necessary. Thus, the effects of ASAP1 on GC cell motility, migration, and invasion were performed by using wound healing assay. It revealed that cells transfected with ASAP1 siRNA were slower to close scratch wounds than control cells (*Figure 2A,D)*.. Furthermore, a transwell assay demonstrated that ASAP1 down-regulation suppressed GC cell migration and invasion compared with control cells (*Figure 2B,E)*.. Western blot analysis revealed that knowdown of ASAP1 in MGC–803 and SGC–7901 cells simultaneously results in down-regulation of the metastasis-related protein levels including MMP–2 and MMP–9 compared with that in NC group cells (*Figure 2C,F)*..

ASAP1 knockdown suppresses cell angiogenesis

We evaluated tube formation after ASAP1 knockdown in both MGC–803 and SGC–7901 GC cells. Tube numbers for each group were observed under a light microscope. As expected, ASAP1 knockdown significantly inhibited tube formation by UHVECs (*Figure 3A, B)*.. Furthermore, it also indicated that VEGF and HIF–1 expression levels were strongly lower in the knockdown group compared with control groups (*Figure 3C,D)*..

ASAP1 regulated EMT in GC cells

Noting that E-cadherin expression lossing, a hallmark of EMT, functions in many malignancies and correlates with higher metastatic potential,[20] we explored the levels of E-cadherin, N-cadherin, Vimentin, Fibronetin, Snail, and Twist protein expression under conditions of ASAP1 knocking down. ASAP1 downregulation surpressed the expression of mesenchymal markers such as N-cadherin, Vimentin, Fibronetin, Snail, and Twist, but in part rescued the expression of epithelial markers like E-cadherin (*Supplementary Figure 3)*..

ASAP1 promotes tumor growth and angiogenesis in vivo

To further evaluate the influence of ASAP1 in vivo experiment, a tumor xenograft model was established in BALB/C nude mice (n = 5 per group) via subcutaneous injection with stable SGC–7901/Control, SGC–7901/NC and SGC–7901/siRNA (ASAP1) clones with more than 80% efficiency, and tumor growth was monitored over a period of 28 days. Marked growth inhibition in vivo was observed in mice inoculated with SGC–7901/siRNA cells compared with that with SGC–7901/Control and SGC–7901/NC cells

(*Figure 4A).*. IHC and Western blot analysis both revealed lower expression level of ASAP1 in tissues of mice inoculated with SGC–7901/siRNA cells compared with other two groups (*Figure 4B,C).*. Analysis of VEGF and HIF–1α protein expression by Western blot showed significantly lower levels of VEGF and HIF–1α in tumors generated from ASAP1 downregulating cells than that in controls, indicating a lower ability of angiogenesis in ASAP1 silence tumors (*Figure 4D,E).*.

Analysis of ASAP1 expression and its clinical significance according to TCGA and GEO databases

As presented in *Figure 5,* ASAP1 showed higher expression in tumor samples than that in normal samples ($P < 0.0001$) according to TCGA database. The GEO database revealed that the higher the malignancy of the disease, the higher the relative expression of ASAP1 ($P = 0.0097$). To further explore the effect of ASAP1 on survival according to TCGA database, we removed all samples with incomplete information and reanalyzed the prognosis. Analysis of the remaining 211 tumor samples (including 105 high ASAP1 expression and 106 low ASAP1 expression) showed that the high expression of ASAP1 presented a poor survival outcome ($P = 0.0362$). In*Figure 5* (TCGA database), high expression of ASAP1 in GC samples was significantly associated with N stage ($P = 0.0271$), T stage ($P = 0.0002$), and pathological stage ($P = 0.0035$). However, no statistical significance was observed between ASAP1 expression and M stage ($P = 0.6170$).

Next, the correlation between ASAP1 and tumor invasion was explored using both the two databases. TCGA database showed that ASAP1 had a statistically positive correlation with 415 invasion-related genes (a total of 513 genes) and had a statistically negative correlation with 51 invasion-related genes (a total 111 of genes). Similar to the above results, the GEO database showed that ASAP1 was a statistically positively correlated with 209 invasion-related genes (a total of 363 genes) and statistically negatively correlated with 60 invasion-related genes (a total of 213 genes).

In addition, TCGA database demonstrated that ASAP1 was statistically positively correlated with 105 angiogenesis-related genes (a total of 132 genes) and was a statistically negatively correlated with 17 angiogenesis-related genes (a total of 37 genes). The GEO database demonstrated that ASAP1 was statistically positively correlated with 58 angiogenesis-related genes (a total of 102 genes) and statistically negatively correlated with 19 angiogenesis-related genes (a total of 54 genes). These results indicate that ASAP1 is associated with the invasion and angiogenesis of GC.

Discussion

Patients with GC metastasis usually have poor prognosis with a short life expectancy. The 5-year survival rate of patients with advanced cancer is 50%, whereas that in early diagnosed cases is 95% [1]. GC has a high mortality, which is associated with delayed diagnosis as a result of the non-specific early disease manifestations and its aggressive nature [26]. Given the insufficient understanding of the molecular

mechanisms that involve GC development, invasion and metastasis, and the diagnosis and prognosis for GC remain challenging. The present study found that ASAP1 expression was upregulated among GC tissues and cell lines, ASAP1 functioned as an oncogene promoting GC cell motility and invasion, angiogenesis, and EMT, suggesting its potential role in GC.

The current study had analyzed the value of ASAP1 level among 625 samples with GC, and the results showed that ASAP1 expression was related to the TNM stage and LNM. According to TCGA database, ASAP1 was associated with the pathological stage, N stage, and T stage in GCs. Hou et al. [27] revealed that ASAP1 level showed a strong correlation with pelvic metastasis in epithelial ovarian cancer. Furthermore, the present study showed that elevated ASAP1 protein expression was independently related to LNM of GCs. In laryngeal squamous cell carcinoma, markedly elevated ASAP1 mRNA expression is related to LNM and the clinical tumor stage [28]. Such findings indicate that increased ASAP1 expression can promote tumor progression and represents an invasive phenotype.

In addition, according to the Kaplan-Meier method, ASAP1 level showed significant association with poor prognosis of GC cases. Univariate and multivariate analyses indicated that ASAP1 level could be used to independently predict the prognosis for GC patients with R0 resection. Normally, cases with node-negative GC are associated with favorable prognosis relative to those with node-positive GC [29]. However, numerous newly diagnosed cases at the advanced stage in China are deprived of the optimal chance of radical surgery [30].With regard to TCGA database, ASAP1 overexpression showed poor survival outcome in tumor samples. ASAP1 alone or ASAP1 is a component involved in tumor cell motility, migration, invasion, and metastasis in metastatic prostate cancer [21], breast cancer [13], and colorectal cancer [19],respectively. A previous study reported that ASAP1 knockdown could inhibit tumor cell malignant grade in vitro; however, the mechanism of ASAP1 in promoting tumor cells had not been comprehensively elucidated. In the present study, ASAP1 knockdown could suppress GC cell (MGC–803 and SGC–7901) motility, migration, and invasion. As far as we knew, the present study is the first to reveal that ASAP1 regulates the malignant behavior of GC cells by upregulating metastasis-related protein (MMP–2 and MMP–9). Furthermore, TCGA and GEO databases revealed that ASAP1 expression was significantly associated with invasion and metastasis-related genes. Therefore, the underlying mechanism of ASAP1 in promoting the invasion and metastasis of cells was identified.

Metastasis is a multi-step process, involving angiogenesis, ECM remodeling, elevated motility, and EMT [31]. Angiogenesis represents an important process during tumor progression [32,33]. TCGA and GEO databases showed that ASAP1 expression was significantly related to tumor angiogenesis. This study is the first to examine the role of ASAP1 in tumor angiogenesis in vitro and in vivo. The results showed that knockdown of ASAP1 reduced angiogenesis. Moreover, knockdown of ASAP1 might directly affect HIF–1α and VEGF degradation among MGC–803 and SGC–7901 cells. HIF–1α is upregulated among various human cancers and promotes tumorigenesis via angiogenesis [34,35]. VEGF is a gene responsive to HIF–1 [36],and its abnormal expression has been recognized as a critical factor that regulates the hypoxia-derived angiogenesis [37]. Thus, the current report is the first to reveal the mechanism of ASAP1 in

inhibiting angiogenesis, which is achieved via the HIF−1α and VEGF pathways, supporting that ASAP1 plays a vital role in promoting tumor angiogenesis.

Tumor metastasis marks a complicated process, which begins with the invasion of primary tumor via the endothelial barrier through the EMT process. This process is featured by the lost adhesion between cells, along with the elevated motility of cells [38,39]. EMT has been recognized as the first step in metastasis; however, the metastatic cells should restore their epithelial status to colonize and form the macrometastases at the sites of metastases [40]. ASAP1 expression promoted EMT by increasing the expression of N-cadherin and vimentin, markers of mesenchymal cells, while decreasing that of E-cadherin, marker of epithelial cells, among ovarian cancer cells [22]. This findng is consistent with our results. Our findings suggested that knocking down ASAP1 can reverse EMT through upregulating the expression of E-cadherin, and downregulating the expression of N-cadherin and vimentin. In addition, downregulating ASAP1 can reverse EMT by reducing Fibronetin, Snail, and Twist. These findings indicated that ASAP1 promotes tumor metastasis through the process of EMT.

Conclusion

ASAP1 may potentially serve as a new prognostic and LNM marker among GC cases. Besides, ASAP1 facilitates angiogenesis by modulating HIF−1α and VEGF pathway and EMT by regulating EMT-associated protein markers, thus promoting the invasion as well as metastasis of GC cells. Our results revealed the pathologic effect of ASAP1 on GC, which can serve as a prognostic predictor and treatment target for GC, and other cancers.

Abbreviations

ASAP1: ArfGAP with SH3 Domain, Ankyrin Repeat and PH Domain 1; GC: gastric cancer; TCGA: The Cancer Genome Atlas; GEO: Gene Expression Omnibus; CRC: colorectal cancer; BC: breast cancer; PCa: prostate cancer; EMT: epithelial-mesenchymal transition; TMAs: tissue microarray; IHC: immunohistochemistry; ATCC: American Type Culture Collection; HUVECs: human umbilical vein endothelial cells; LNM: lymph node metastasis; SD: standard deviation; OR: odds ratio; CI: confidence interval; OS: overall survival.

Declarations

Funding

This study was supported by the Fundamental Research Funds for the Provincial Universities (2017LCZX71), Nn10 program of Harbin Medical University Cancer Hospital (Nn10PY2017−03), the Key Projects of Haiyan Foundation of Harbin Medical University Cancer Hospital (JJZD2019−02), the Youth Elite Training Foundation of Harbin Medical University Cancer Hospital (JY2016−03), and the Outstanding youth fund of Harbin Medical University Cancer Hospital (JCQN2019−06).

Availability of data and materials

All data generated or analysed during this study are included in this published article [and its supplementary information files].

Authors' contributions

Conception and design: HY. G., TB. L. and YW. X.; data production, analysis and interpretation: HY. G., L. Q., HW. S., HB. S., and ZG. L.; writing the manuscript: HY. G., HF. Z., CF. L., and Y. M. All authors reviewed the manuscript and accepted the content.

Ethics approval and consent to participate

GC tissues were collected from patients who underwent surgical resection at the Harbin Medical University Cancer Hospital (Harbin, China). All patients signed consent letters and all manipulation of the tissues was approved by the Ethics Committee of Harbin Medical University Cancer Hospital. All experiments were performed in accordance with the guidelines of the Harbin Medical University.

Consent for publication

We have obtained consents to publish this paper from all the participants of this study.

Competing interests

The authors declare that they have no competing interests.

References

1. Ferro A, Peleteiro B, Malvezzi M, Bosetti C, Bertuccio P, Levi F, et al. Worldwide trends in gastric cancer mortality (1980-2011), with predictions to 2015, and incidence by subtype. Eur J Cancer. 2014;50:1330-44.

2. Torre LA, Bray F, Siegel RL, Ferlay J, Lortet-Tieulent J, Jemal A. Global cancer statistics, 2012. CA Cancer J Clin. 2015;65:87-108.

3. Arnold M, Moore SP, Hassler S, Ellison-Loschmann L, Forman D, Bray F. The burden of stomach cancer in indigenous populations: a systematic review and global assessment. Gut. 2014;63:64-71.

4. Zhu X, Li J. Gastric carcinoma in China: Current status and future perspectives (Review). Oncol Lett. 2010;1:407-412.

5. Marrelli D, De Stefano A, de Manzoni G, Morgagni P, Di Leo A, Roviello F. Prediction of recurrence after radical surgery for gastric cancer: a scoring system obtained from a prospective multicenter study. Ann Surg. 2005;241:247-55.

6. Kim S, Lim DH, Lee J, Kang WK, MacDonald JS, Park CH, et al. An observational study suggesting clinical benefit for adjuvant postoperative chemoradiation in a population of over 500 cases after gastric resection with D2 nodal dissection for adenocarcinoma of the stomach. Int J Radiat Oncol Biol Phys. 2005;63:1279-85.

7. van HagenP, Hulshof MC, van Lanschot JJ, Steyerberg EW, van Berge Henegouwen MI, Wijnhoven BP, et al. Preoperative chemoradiotherapy for esophageal or junctional cancer. N Engl J Med. 2012;366:2074-84.

8. Ferlay J, Soerjomataram I, Ervik M, Dikshit R, et al. GLOBOCAN 2012 v1.0, Cancer incidence and mortality worldwide: IARC CancerBase No. 11. 2012[cited 2016 January 25]. http://globocan. iarc.fr.

9. Crew KD, Neugut AI. Epidemiologyof gastric cancer. World J Gastroenterol. 2006;12:354-62.

10. Wagner AD, Grothe W, Haerting J, Kleber G, Grothey A, Fleig WE. Chemotherapyin advanced gastric cancer: a systematic review and meta-analysis based on aggregate J Clin Oncol. 2006;24:2903-9.

11. Bharti S, Inoue H, Bharti K, Hirsch DS, Nie Z, Yoon HY, Artym V, et al. Src-dependent phosphorylation of ASAP1 regulates podosomes. Mol Cell Biol. 2007;27:8271-83.

12. Liu Y, Yerushalmi GM, Grigera PR, Parsons JT. Mislocalization or reduced expression of Arf GTPase-activating protein ASAP1 inhibits cellspreading and migration by influencing Arf1 GTPase cycling. J Biol Chem. 2005;280:8884-92.

13. Onodera Y, Hashimoto S, Hashimoto A, Morishige M, Mazaki Y, Yamada A, et al. Expression of AMAP1, an ArfGAP, provides novel targets to inhibit breast cancer invasiveactivities. EMBO J. 2005;24:963-73.

14. Randazzo PA, Andrade J, Miura K, Brown MT, Long YQ, Stauffer S, et al. The Arf GTPase-activating protein ASAP1 regulates the actin cytoskeleton. Proc Natl Acad Sci U S A. 2000;97:4011-6.

15. Liu Y, Loijens JC, Martin KH, Karginov AV, Parsons JT. The association of ASAP1, an ADP ribosylation factor-GTPase activating protein, with focal adhesion kinase contributes to the process of focal adhesion assembly. Mol Biol Cell. 2002;13:2147-56.

16. Oda A, Wada I, Miura K, Okawa K, Kadoya T, Kato T, et al. CrkL directs ASAP1 to peripheral focal adhesions. J Biol Chem. 2003;278:6456-60.

17. Randazzo PA, Inoue H, Bharti S. Arf GAPs as regulators of the actin cytoskeleton. Biol Cell. 2007;99:583-600.

18. Furman C, Short SM, Subramanian RR, Zetter BR, Roberts TM. DEF-1/ASAP1 is a GTPase-activating protein (GAP) for ARF1 that enhances cell motility through a GAP-dependent mechanism. J Biol Chem. 2002;277:7962-9.

19. Müller T, Stein U, Poletti A, Garzia L, Rothley M, Plaumann D, et al. ASAP1 promotes tumor cell motility and invasiveness, stimulates metastasis formation in vivo, and correlates with poor survival in colorectal cancer patients. Oncogene. 2010;29:2393-403.

20. Ehlers JP, Worley L, Onken MD, Harbour JW. DDEF1 is located in an amplified region of chromosome 8q and is overexpressed in uveal melanoma. Clin Cancer Res. 2005;11:3609-13.

21. Lin D, Watahiki A, Bayani J, Zhang F, Liu L, Ling V, et al. ASAP1, a gene at 8q24, is associated with prostate cancer metastasis. Cancer Res. 2008;68:4352-9.

22. Zhang T, Zhao G, Yang C, Dong P, Watari H, Zeng L, et al. Lentiviral vector mediated-ASAP1 expression promotes epithelial to mesenchymal transition in ovarian cancer cells. Oncol Lett. 2018;15:4432-4438.

23. Sato H, Hatanaka KC, Hatanaka Y, Hatakeyama H, Hashimoto A, Matsuno Y, et al. High level expression of AMAP1 protein correlates with poor prognosis and survival aftersurgery of head and neck squamous cell carcinoma patients. Cell Commun Signal. 2014;12:17.

24. Sobin L, Gospodarowicz M, Wittekind C, editors. TNM Classification of Malignant Tumours (UICC International Union Against Cancer). 7th ed. New York: Wiley-Blackwell; 2009.

25. Dhawan A, Scott JG, Harris AL, Buffa FM. Pan-cancer characterisation of microRNA across cancer hallmarks reveals microRNA-mediated downregulation of tumour suppressors. Nat Commun. 2018; 9:5228.

26. Xie K, Huang S. Regulation of cancer metastasis by stress pathways. Clin Exp Metastasis. 2003;20:31-43.

27. Hou T, Yang C, Tong C, Zhang H, Xiao J, Li J. Overexpression of ASAP1 is associated with poor prognosis in epithelial ovarian cancer. Int J Clin Exp Pathol. 2013;7:280-7.

28. Li M, Tian L, Yao H, Lu J, Ge J, Guo Y, et al. ASAP1 mediates the invasive phenotype of human laryngeal squamous cell carcinoma to affect survival prognosis. Oncol Rep. 2014;31:2676-82.

29. Jeuck TL, Wittekind C. Gastric carcinoma: stage migration by immunohistochemically detected lymph nodemicrometastases. Gastric Cancer. 2015;18:100-8.

30. Lin Y, Ueda J, Kikuchi S, Totsuka Y, Wei WQ, Qiao YL, et al. Comparative epidemiology of gastric cancer between Japan and China. World J Gastroenterol. 2011;1:4421-8.

31. Hur K, Toiyama Y, Takahashi M, Balaguer F, Nagasaka T, Koike J, et al. MicroRNA-200c modulates epithelial-to-mesenchymal transition (EMT) in human colorectal cancer metastasis. Gut. 2013;62:1315-26.

32. Zhu J, Sheng J, Dong H, Kang L, Ang J, Xu Z. Phospholipid scramblase 1 functionally interacts with angiogenin and regulates angiogenin-enhanced rRNA transcription. Cell Physiol Biochem. 2013;32:1695-706.

33. Zhu X, Er K, Mao C, Yan Q, Xu H, Zhang Y, et al. miR-203 suppresses tumor growth and angiogenesis by targeting VEGFA in cervical cancer. Cell Physiol Biochem. 2013;32:64-73.

34. Semenza GL. HIF-1 and tumor progression: pathophysiology and therapeutics. Trends Mol Med. 2002;8:S62-7.

35. Semenza GL. HIF-1: using two hands to flip the angiogenic switch. Cancer Metastasis Rev. 2000;19:59-65.

36. Stacker SA, Caesar C, Baldwin ME, Thornton GE, Williams RA, Prevo R, et al. VEGF-D promotes the metastatic spread of tumor cells via the lymphatics. Nat Med. 2001;7:186-91.

37. Goel HL, Mercurio AM. VEGFtargets the tumour cell. Nat Rev Cancer. 2013;13:871-82.

38. Acloque H, Adams MS, Fishwick K, Bronner-Fraser M, Nieto MA. Epithelial-mesenchymal transitions: the importance of changing cell state in development and disease. J Clin Invest. 2009;119:1438-49.

39. Zavadil J, Böttinger EP. TGF-betaand epithelial-to-mesenchymal Oncogene. 2005;24:5764-74.

40. Tse JC, Kalluri R. Mechanisms of metastasis: epithelial-to-mesenchymal transition and contribution of tumor microenvironment. J Cell Biochem. 2007;101:816-29.

Tables

Table 1. The correlation of clinicopathologic features with the expression of ASAP1 in GC

Variables	Total N=625	ASAP1 protein expression status		*P*
		Low (%)	High (%)	
Age (years)				0.744
≤ 58	325	205 (63.1)	120 (36.9)	
> 58	300	193 (64.3)	107 (35.7)	
Gender				0.328
Male	471	305 (64.8)	166 (345.2)	
Female	154	93 (60.4)	61 (39.6)	
Main location				0.879
Upper	430	275 (64.0)	155 (36.0)	
Middle	137	85 (62.0)	52 (38.0)	
Lower	58	38 (65.5)	20 (34.5)	
Tumor size (cm)				0.910
≤ 5	313	200 (63.9)	113 (36.1)	
> 5	312	198 (63.5)	114 (36.5)	
TNM stage				< 0.0001
I/II	197	152 (77.2)	45 (22.8)	
III/IV	428	246 (57.5)	182 (42.5)	
Depth of invasion				0.791
T1/T2	158	102 (64.6)	56 (35.4)	
T3/T4	467	296 (63.4)	171 (36.6)	
Lymph node metastasis				< 0.0001
Negative	153	125 (81.7)	28 (18.3)	
Positive	472	273 (57.8)	199 (42.2)	
Borrmann grouping				0.542
I	37	26 (70.3)	11 (29.7)	
II	171	108 (63.2)	63 (36.8)	
III	342	221 (64.6)	121 (35.4)	
IV	75	43 (57.3)	32 (42.7)	
Lauren classification				0.983

Intestinal	297	189 (63.6)	108 (36.4)	
Diffuse	328	209 (63.7)	119 (36.3)	
Resectability				0.325
R0	490	317 (64.7)	173 (35.3)	
R1	38	20 (52.6)	18 (47.3)	
R2	97	61 (62.9)	36 (37.1)	

TNM, tumor, node, and metastasis system.

Table 2. Multivariate analysis of the association between ASAP1 expression and lymph node metastasis

Variable		B	S.E.	*P*	OR	95%CI
TNM stage	I/II					
	III/IV	1.637	0.154	< 0.0001	5.138	3.797-6.953
Resectability	R0			0.024		
	R1	0.653	0.743	0.379	1.922	0.448-8.246
	R2	2.045	0.785	0.009	7.731	1.660-36.007
ASAP1 expression	Low					
	High	1.117	0.289	0.0001	3.005	1.734-5.383

B and SE are the parameter estimator of association coefficient and its standard error, respectively; OR, odds ratio; CI, confidence interval

Figures

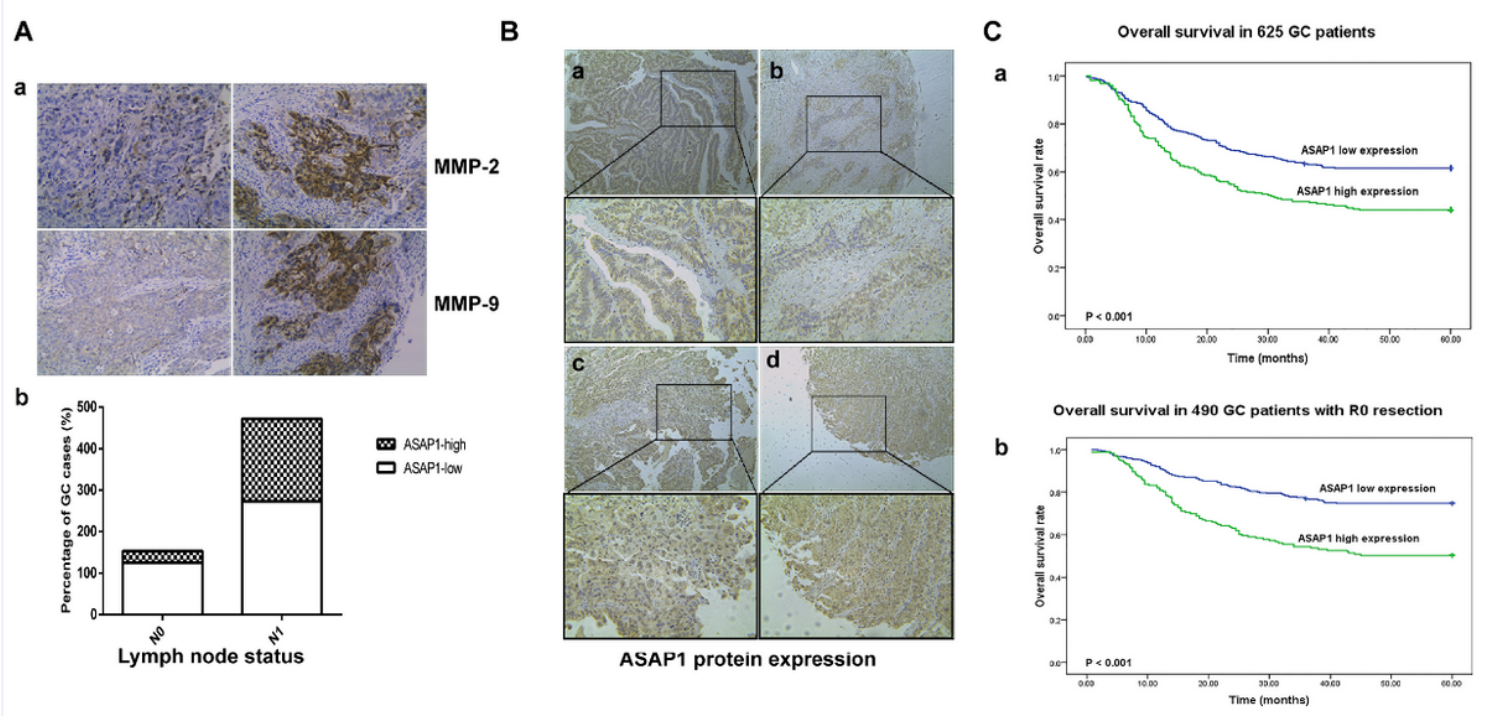

Figure 1

Elevated ASAP1 expression in GC patients is associated with lymph node metastasis and poor survival. A: (a) IHC analysis MMP-2 and MMP-9 expression in GC patients, (b) Patients were classified in two groups, i.e., with (N1) or without (N0) lymph node metastasis. B: Representative IHC images of ASAP1 expression in GC tissue microarrays. C: Kaplan–Meier curves of the overall survival (OS) for gastric cancer patients with high and low ASAP1 expression.

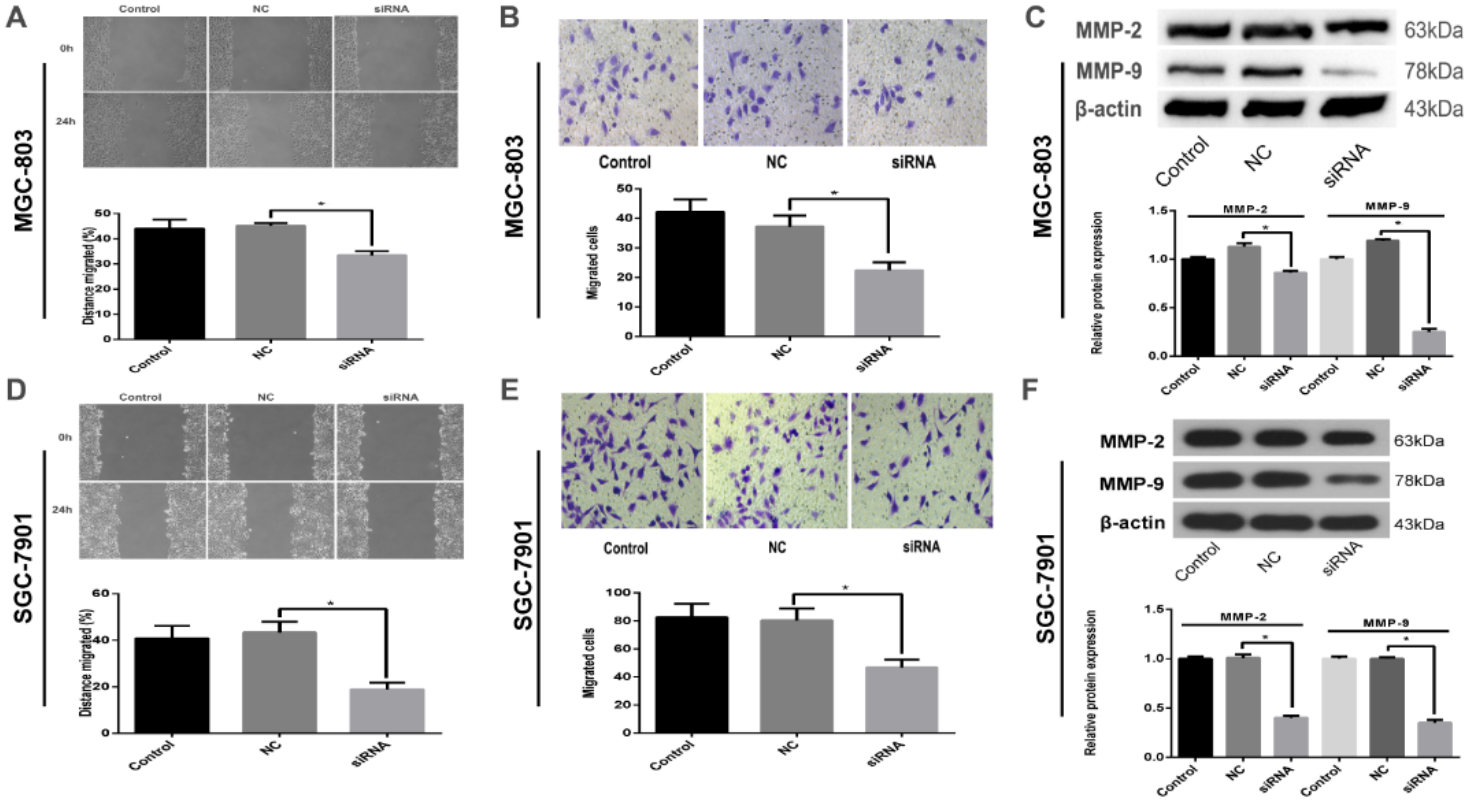

Figure 2

ASAP1 increases the motility and invasive properties of gastric cancer cells. Wound healing assays were used to examine the migration of MGC-803 (A) and SGC-7901 (D) cells. Inhibition of ASAP1 dramatically reduced the migration capacity of both tumor cells. (*P = 0.0005 and *P = 0.0015) The migration and invasion of MGC-803 (B) and SGC-7901 (E) cell lines were measured in a transwell assay. Inhibition of ASAP1 significantly reduced the cells' invasion capacity. (*P < 0.0001 and *P < 0.0001) Western blot analysis showed that ASAP1 promotes metastasis-associated protein (MMP-2 and MMP-9) expression in MGC-803 (C) (*P = 0.0003 and *P < 0.0001) and SGC-7901 (F) cells (*P < 0.0001 and *P < 0.0001).

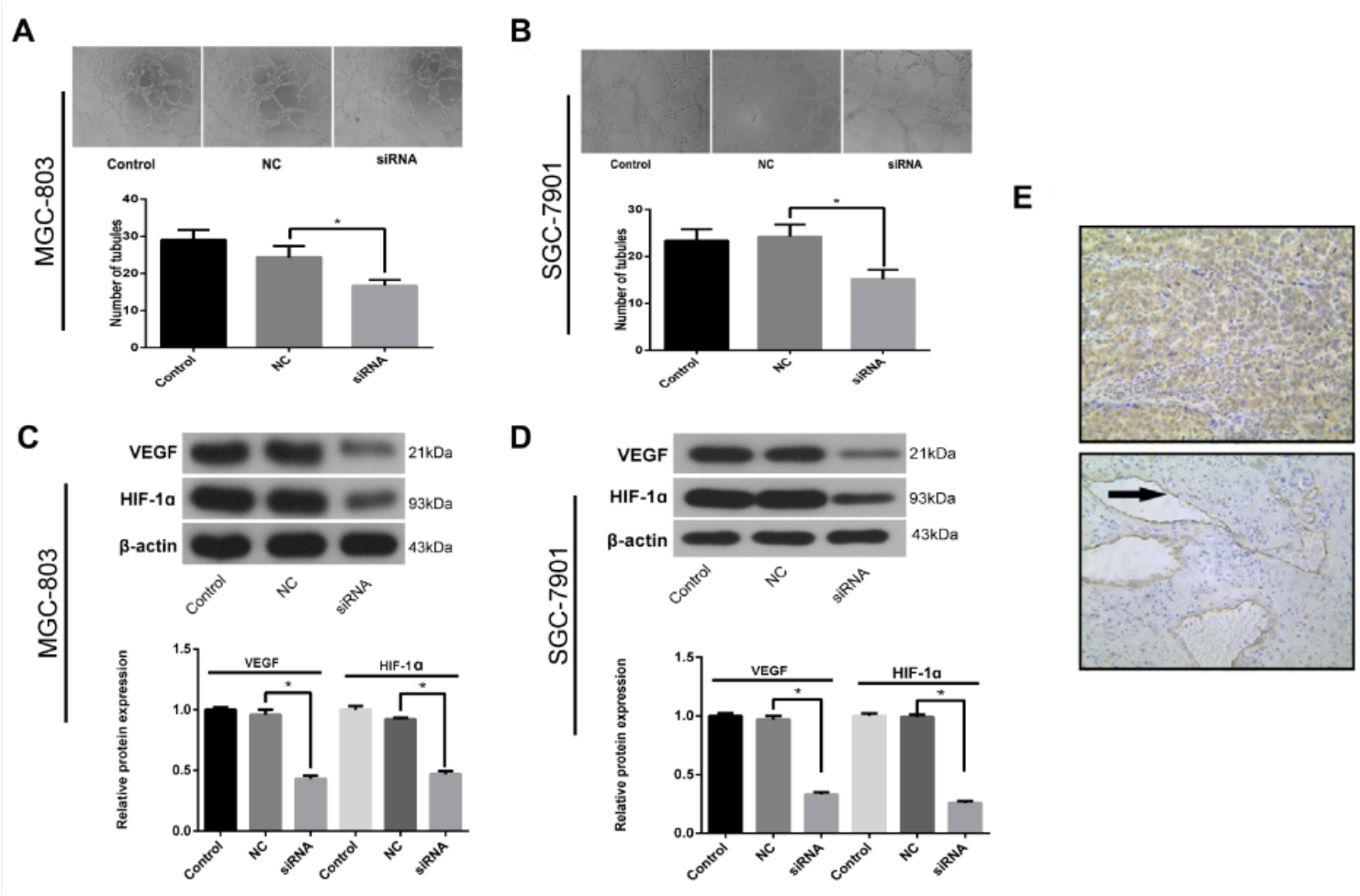

Figure 3

ASAP1 is involved in gastric cancer angiogenesis. ASAP1 knockdown significantly suppressed tube formation by HUVECs in MGC-803 (A) and SGC-7901 (B) cells. (*P = 0.0179 and *P = 0.0084) Western blot analysis showed that ASAP1 promotes angiogenesis-associated protein (VEGF and HIF-1) expression in MGC-803 (C) (*P < 0.0001 and *P < 0.0001) and SGC-7901 (D) (*P < 0.0001 and *P < 0.0001) cells. E: Immunohistochemical anlaysis of (a) ASAP1 protein high expression and (b) CD31 high expression in the same gastric cancer tissues.

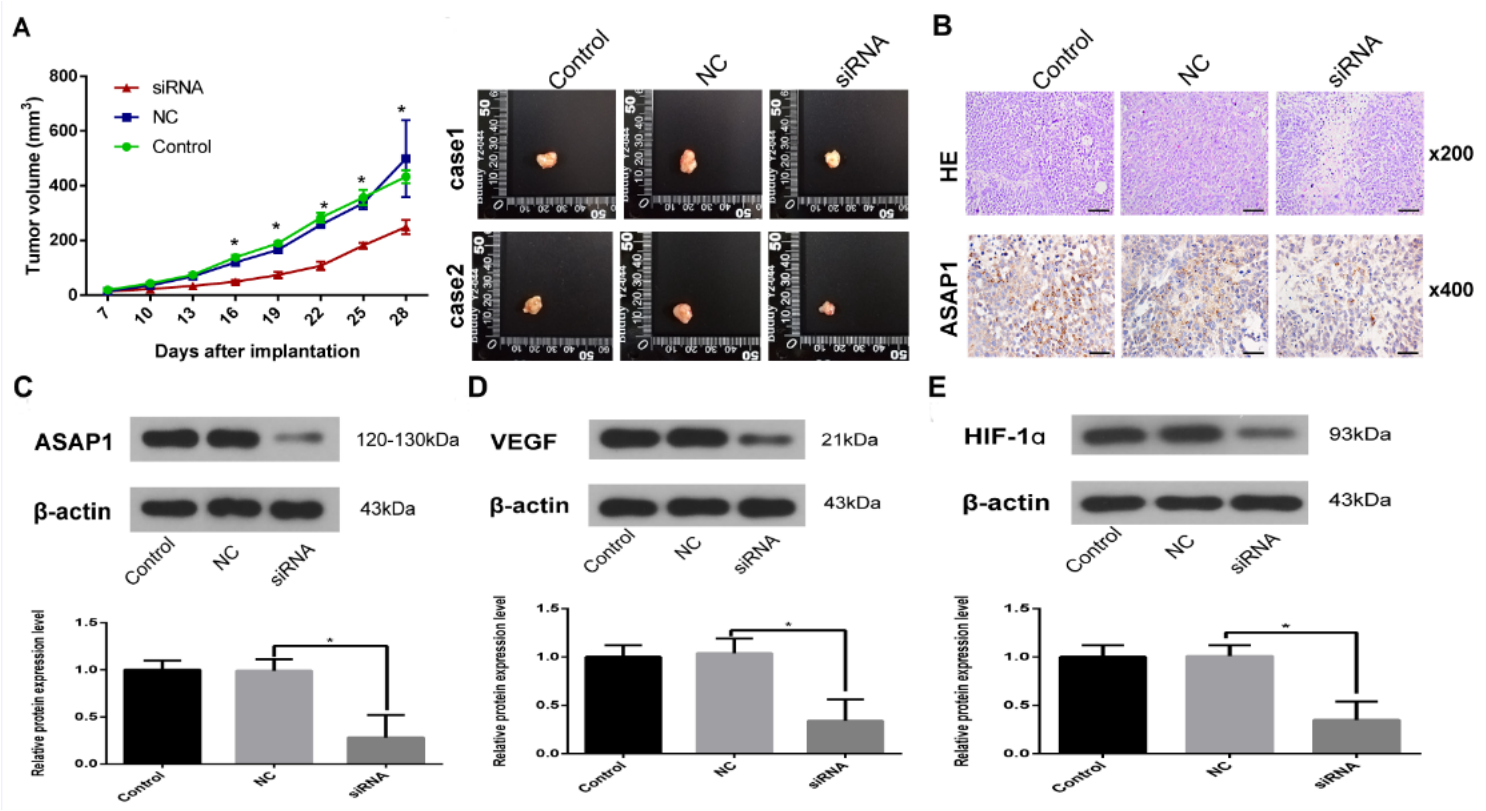

Figure 4

ASAP1 promotes SGC-7901 xenograft tumor growth and angiogenesis in nude mice. A: Tumor volumes over 28 days of observation. Knockdown of ASAP1 led to a marked reduction in tumor volume. (*P(16) = 0.0005, *P(19) = 0.0012, *P(22) = 0.0003, *P(25) = 0.0013, and *P(28) = 0.0023) B: Representative images of hematoxylin and eosin (H&E) and immunohistochemical staining in gastric tissues of mice injected with SGC-7901/Control, SGC-7901/NC and SGC-7901/ASAP1 siRNA are shown. Representative western blot showing the effects of ASAP1 (C) on the expression of VEGF (D) and HIF-1α (E) in gastric cancer cells. (*P = 0.0102, *P = 0.0065 and *P = 0.0104).

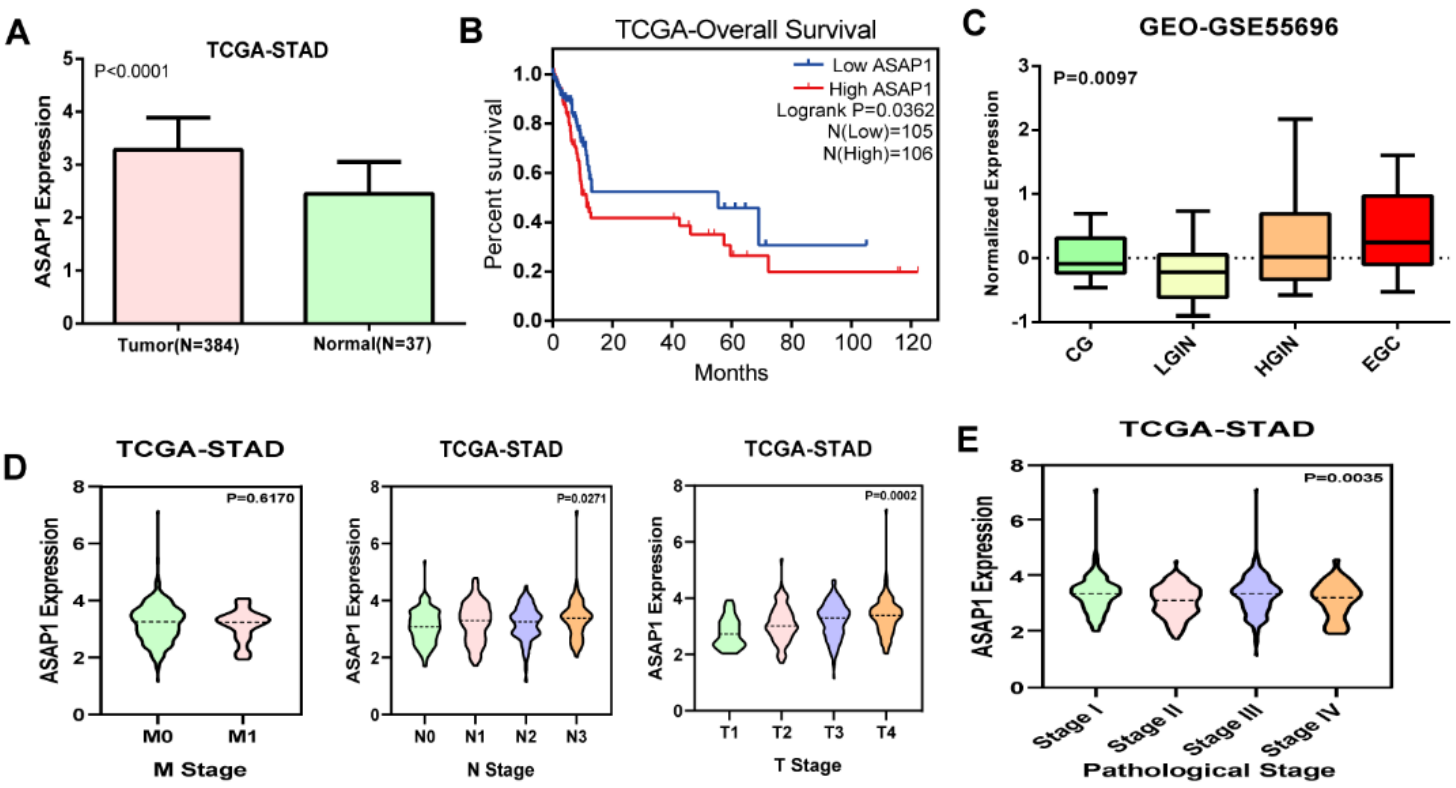

Figure 5

The expression data of ASAP1 based on TCGA and GEO datasets. A: ASAP1 expression levels in tumor samples (n=384) and normal samples (n=37) from TCGA database were analyzed. B: Survival analysis for patients with low or high expression levels of ASAP1. C: ASAP1 expression levels in 19 chronic gastritis (CG), 19 low-grade intraepithelial neoplasia of stomach (LGIN), 20 high-grade intraepithelial neoplasia stomach (HGIN), and 19 early gastric cancer (EGC) samples based on GEO data base. D: ASAP1 expression levels in different TNM stage in GC according to TCGA database. E: Association between ASAP1 expression and pathological stage according to TCGA database.

Supplementary Files

This is a list of supplementary files associated with this preprint. Click to download.

- SupplementaryFigure1.tif
- SupplementaryFigure2.tif
- SupplementaryFigure3.tif
- SupplementaryTable1.docx
- GSE55696SustainedAngiogenesisGeneCorASAP1.xls
- SupplementaryTable2.docx